

# NMDA and Non-NMDA Receptor-mediated Increase of *c-fos* mRNA in Dentate Gyrus Neurons Involves Calcium Influx via Different Routes

Leslie S. Lerea,<sup>1</sup> Linda S. Butler,<sup>1</sup> and James O. McNamara<sup>1,2</sup>

<sup>1</sup>Department of Medicine, Division of Neurology, and <sup>2</sup>Departments of Pharmacology and Neurobiology and Epilepsy Research Laboratory, Veterans Administration Medical Center, Duke University, Durham, North Carolina 27710

We examined the effects of selective agonists of ionotropic excitatory amino acid (EAA) receptor subtypes on induction of the immediate early gene *c-fos*. We used *in situ* hybridization to measure *c-fos* mRNA and fura-2 imaging to measure intracellular calcium ( $Ca^{2+}$ ) in individual dentate gyrus neurons maintained *in vitro*. Activation of either NMDA or non-NMDA receptor subtypes is sufficient to induce the rapid and dramatic increase of *c-fos* mRNA. Activation of either NMDA or non-NMDA receptors also induces a rapid and dramatic increase of  $Ca^{2+}$ , effects blocked by the removal or chelation of extracellular calcium ( $Ca^{2+}$ ). *c-fos* mRNA induction by either receptor subtype is  $Ca^{2+}$  dependent, since chelation of  $Ca^{2+}$  with EGTA prevents *c-fos* mRNA induction by both NMDA and non-NMDA receptor agonists. The increase in  $Ca^{2+}$  induced by activating non-NMDA receptors is inhibited either by removal of extracellular sodium ( $Na^+$ ) or by the voltage-sensitive calcium channel (VSCC) blocker nifedipine. By contrast, the increase of  $Ca^{2+}$  induced by activating NMDA receptors is not inhibited by removal of  $Na^+$  or nifedipine. Consistent with these effects on  $Ca^{2+}$ , nifedipine inhibits induction of *c-fos* mRNA by non-NMDA, but not by NMDA, receptor agonists. These findings indicate that  $Ca^{2+}$  serves as a second messenger coupling ionotropic EAA receptors with transcriptional activation of *c-fos* mRNA. The route of  $Ca^{2+}$  entry into dentate neurons, however, depends on the EAA receptor subtype stimulated. Non-NMDA receptor activation results in  $Ca^{2+}$  influx indirectly via VSCCs, whereas NMDA receptor activation results in  $Ca^{2+}$  influx directly through the NMDA channel itself. Since non-NMDA and NMDA receptors are colocalized at some synapses and can be activated simultaneously by synaptically released glutamate, the induction of *c-fos* mRNA by each receptor may reflect the activation of identical and therefore redundant programs of gene expression. Alternatively, the varying routes of  $Ca^{2+}$  entry following stimulation of EAA receptor subtypes may activate distinct signaling pathways that cul-

minate in different programs of early gene expression and correspondingly different patterns of target gene expression.

The molecular mechanisms by which brief experiences produce lasting modifications of nervous system function are unknown. Long-term changes could be due to posttranslational modifications of existing proteins and/or alterations in gene expression. Immediate-early genes (IEGs) such as *c-fos* have been implicated in the conversion of short-term stimuli to long-term alterations in cellular phenotype by regulating gene expression (Curran and Morgan, 1985; Goelet et al., 1986; Morgan and Curran, 1989). Activation of glutamate receptors is critical to some long-lasting forms of neuronal plasticity. Transient activation of both the NMDA and non-NMDA subtypes of glutamate receptor have been linked to induction of long-term potentiation (Collingridge et al., 1983; Harris et al., 1984; Aniksztejn and Ben-Ari, 1991). Transient activation of the NMDA receptor also is necessary for induction of the long-lasting hyperexcitability in the kindling model of epilepsy (McNamara et al., 1988; Stasheff et al., 1989).

The stimulus necessary for induction of kindling, a brief seizure, is sufficient to induce rapid and dramatic increases of mRNA of multiple IEGs, including *c-fos* (Dragunow and Robertson, 1987; Shin et al., 1990). Activation of the NMDA subtype of glutamate receptor during kindled seizures is necessary for the full induction of *c-fos* mRNA, since NMDA receptor antagonists inhibit seizure induction of *c-fos* mRNA by 50–70% (Labiner et al., 1990). NMDA receptor antagonists also inhibit induction of *c-fos* in other paradigms (Herrera and Robertson, 1990). Activation of the NMDA receptor subtype is sufficient to induce expression of *c-fos in vitro*, but the mechanism by which NMDA produces this effect is unknown (Szekely et al., 1989). The  $Ca^{2+}$  dependence of depolarization-induced increases of *c-fos* mRNA in PC12 cells (Morgan and Curran, 1986) together with the permeability of the NMDA receptor to  $Ca^{2+}$  (Macdermott et al., 1986; Ascher and Nowak, 1988; Iino et al., 1990) suggested that  $Ca^{2+}$  might serve as the second messenger coupling this receptor to *c-fos* mRNA induction.

We examined the effects of selective activation of the ionotropic subtypes of glutamate receptors on *c-fos* mRNA. We used an *in vitro* neuronal cell system, derived from postnatal rat dentate gyrus, to address the following questions: (1) is activation of either NMDA or non-NMDA receptors sufficient to induce *c-fos* mRNA expression; (2) is  $Ca^{2+}$  the second messenger that links activation of these receptors to *c-fos* mRNA expres-

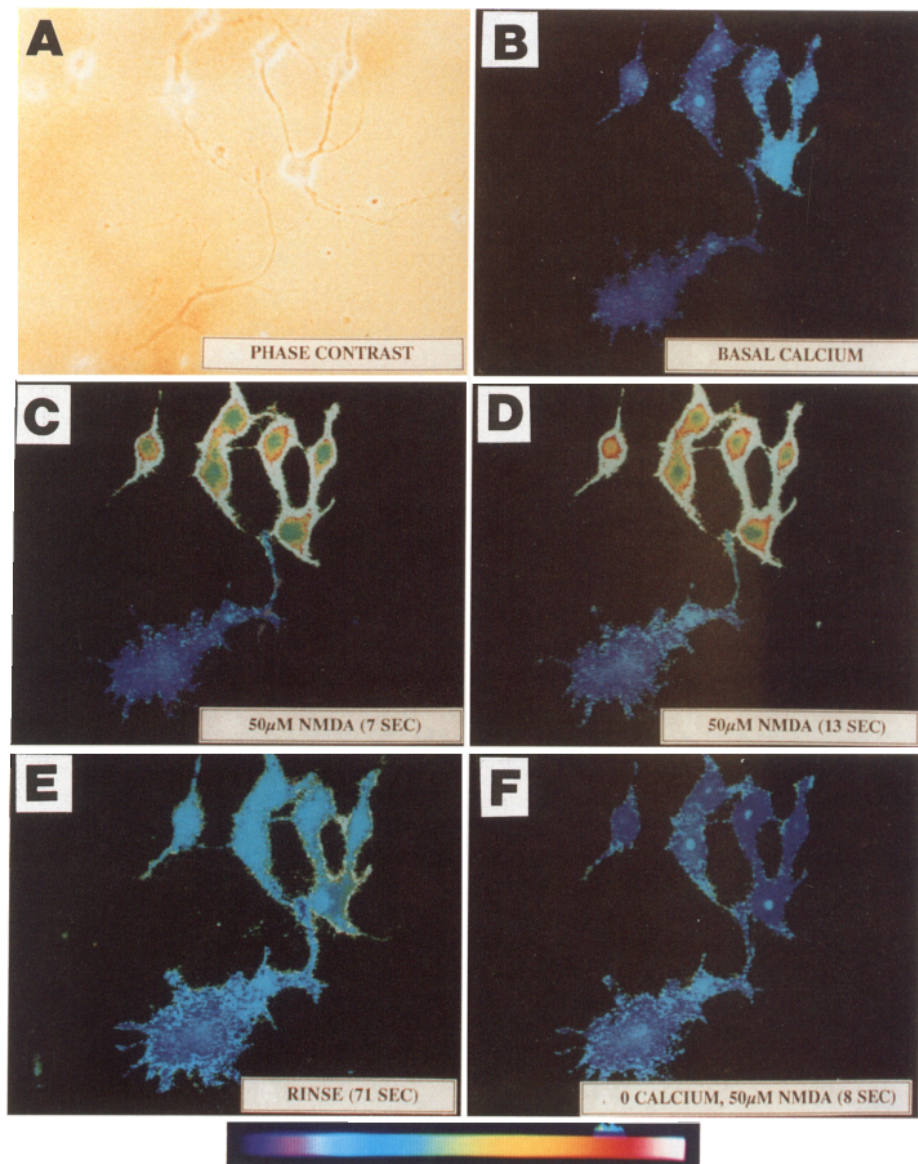
Received July 30, 1991; revised Feb. 5, 1992; accepted Mar. 10, 1992.

We are grateful to Dr. Ken McCarthy for the generous use of the image analysis system for all of the calcium studies. We thank Drs. Doug Bonhaus and Jim Burke for helpful advice and discussions. This study was supported by NIH Grants GM 12049 and NS 17771 and by a grant from the Veterans Administration.

Correspondence should be addressed to Dr. Leslie S. Lerea, Department of Medicine, Box 3676, 401 Bryan Research Building, Duke University, Durham, NC 27710.

Copyright © 1992 Society for Neuroscience 0270-6474/92/122973-09\$05.00/0

**Figure 1.** NMDA-stimulated changes in fura-2 fluorescence in cultured dentate gyrus cells. Pseudocolor-enhanced pictures showing  $\text{Ca}^{2+}$  responses in dentate gyrus neurons following application of NMDA. Dentate gyrus cells loaded with fura-2 were stimulated with  $50 \mu\text{M}$  NMDA, and changes in the fura-2 fluorescence ratio were monitored using a dual-wavelength imaging system with excitation at 350 and 380 nm. The color bar ranges from purple to white and reflects  $\text{Ca}^{2+}$  levels from approximately 50 to 500 nM. *A*, Phase-contrast photomicrograph of the field of cells being studied. Cells are maintained in buffer containing 2 mM  $\text{Ca}^{2+}$  unless otherwise specified. *B*, Pseudocolor representation of ratioed images prior to NMDA. Basal  $\text{Ca}^{2+}$  levels within dentate cells ranged from 50 to 70 nM. *C* and *D*, Pseudocolor representations of ratioed images of fura-2 fluorescence, 7 and 13 sec following addition of NMDA.  $\text{Ca}^{2+}$  increased to 300–400 nM in all neurons in response to NMDA. *E*, Pseudocolor representation of ratioed images 71 sec after NMDA was washed out of the bath. *F*, Pseudocolor representation of ratioed images 8 sec after NMDA addition in  $\text{Ca}^{2+}$ -free buffer. Note the lack of an increase in  $\text{Ca}^{2+}$  when cells are stimulated in the absence of  $\text{Ca}^{2+}$ .



sion; and (3) if so, does  $\text{Ca}^{2+}$  originate from a single source and gain access to the neuron via similar routes?

## Materials and Methods

**Cell preparation.** Dentate gyrus cells were obtained from 4-d-old rat pups according to the method of Mattson and Kater (1989) and maintained for 7–9 d *in vitro* prior to use. Briefly, each hippocampus was dissected and sectioned into 600–800- $\mu\text{m}$ -thick transverse slices using a McIlwain tissue chopper. The dentate gyrus was separated from the hippocampal gyrus by microdissection using a dissecting microscope. Efforts were made to dissect as close to the hilar border of the granule cell layer as possible, thereby excluding the hilus. All tissue was enzymatically dissociated with 0.25% trypsin for 30 min at 37°C. Following trypsinization, tissue was rinsed and dispersed into a single cell suspension by gentle passage through a fire-polished Pasteur pipette. The cell suspension was centrifuged for 10–12 min at  $100 \times g$  and the pellet resuspended in Modified Eagle's Medium supplemented with 33 mM glucose, 1 mM pyruvic acid, 2 mM  $\text{CaCl}_2$ , 15 mM KCl, and 10% fetal calf serum (MEM-C). An estimate of viable cells was obtained using the trypan blue dye exclusion test. Cells were plated in a small volume at a density of  $4\text{--}6 \times 10^3$  cells/ $\text{mm}^2$  onto poly-D-lysine-coated glass chamberslides or 22 mm glass coverslips. Cells were allowed to settle and adhere for several hours prior to adding additional MEM-C. Cells were maintained at 37°C in a humidified incubator with 5%  $\text{CO}_2$ , 95%  $\text{O}_2$ .

**Immunocytochemistry.** Cells were processed for immunocytochemistry according to the protocol of Lerea and McCarthy (1990). Mouse monoclonal antibody against neurofilament was generously supplied by John Woods (Sandoz Laboratories, London, England). Sheep anti-glutamic acid decarboxylase (anti-GAD) antiserum was generously supplied by Don Schmechel (Duke University, Durham, NC). Rabbit anti-glial fibrillary acidic protein (anti-GFAP) antiserum was purchased from Accurate Laboratories (Westbury, NY). Fluorescein isothiocyanate (FITC)-conjugated rabbit anti-sheep IgG, FITC-conjugated goat anti-rabbit IgG, and rhodamine-conjugated goat anti-mouse IgG were purchased from Cappel Laboratories (West Chester, PA).

**Calcium measurements.** The  $\text{Ca}^{2+}$ -sensitive indicator dye fura-2 (Molecular Probes) was used to monitor changes in intracellular calcium ( $\text{Ca}^{2+}$ ) in individual cells as described by McCarthy and Salm (1991). Dentate gyrus cells grown on glass coverslips were loaded with 5  $\mu\text{M}$  fura-2 acetoxymethyl ester in growth media for 30–45 min at 37°C. The coverslip was mounted into a viewing chamber and cells were rinsed with HBSS+ ( $\text{Ca}^{2+}$ /Mg $^{2+}$ /phenol red-free Hanks' Balanced Salt Solution supplemented with 2 mM  $\text{CaCl}_2$  and 5  $\mu\text{M}$  glycine). Fura-2 loading under these conditions yielded a uniform fluorescence within the cells. The cells were visualized on a color monitor with a Zeiss ICM 405 microscope interfaced with an imaging system via an ISIT video camera. Background fluorescence was measured at both 350 nm and 380 nm excitation wavelengths and subtracted from cellular fluorescence during the course of data collection. Ratioed images (350/380 nm) were displayed as 256 pseudocolor-enhanced gray levels. Sixteen images were

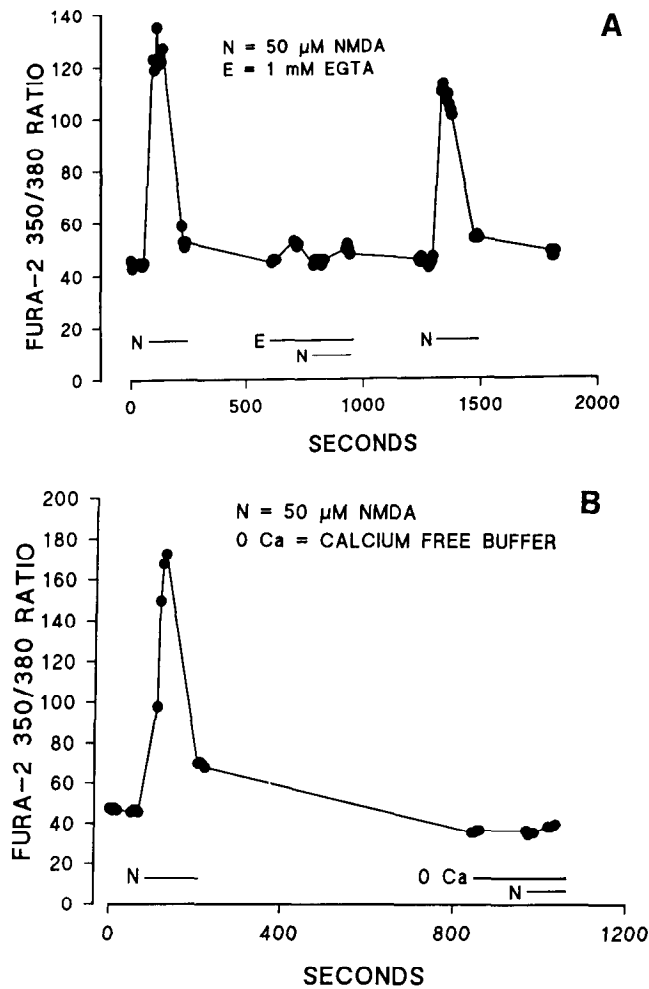


**Figure 2.** Effects of EGTA and 0 extracellular calcium on the NMDA-stimulated calcium response. *A*, Fura-2-loaded dentate gyrus cells were stimulated with NMDA ( $50 \mu\text{M}$ ) in the presence of  $\text{Ca}^{2+}$  ( $2 \text{ mM}$ ), rinsed, and allowed to recover for 15 min. The same cells were restimulated with NMDA in the presence of  $1 \text{ mM}$   $\text{Ca}^{2+}$  plus  $1 \text{ mM}$  EGTA. Cells were rinsed, returned to  $\text{Ca}^{2+}$ -containing buffer, allowed to recover, and restimulated a third time with NMDA. Fura-2 350:380 nm ratios were collected at the times indicated. Values shown are from a single representative cell obtained from a cursor box placed over the ratioed image of the cell. This response is representative of data collected from 20 individual neurons. The bars indicate addition of agonist or drug to the buffer. The fura-2 350/380 ratio refers to the mean, background corrected, 350:380 nm ratio. *B*, Fura-2-loaded dentate gyrus cells were stimulated with NMDA in the presence of  $\text{Ca}^{2+}$  ( $2 \text{ mM}$ ), rinsed, and allowed to recover for 15 min. The same cells were then placed in  $\text{Ca}^{2+}$ -free buffer and restimulated with NMDA. Fura-2 350:380 nm ratios were collected at the times indicated. The bars indicate addition of agonist or drug to the buffer. Values shown are from a single representative cell ( $n = 6$ ).

collected at each wavelength for each field of cells. The images were averaged and background fluorescence at each wavelength subtracted prior to collecting ratios. All experiments were done in  $\text{Mg}^{2+}$ -free HBSS<sup>+</sup> buffer. Vehicle or drug was added directly to the chamber bath as  $10\times$  stock concentrations and changes in the 350/380 nm fura-2 ratio monitored. All fura-2 experiments were done at room temperature. Following stimulation, cells were rinsed three times consecutively in HBSS<sup>+</sup> and allowed at least a 15 min recovery period prior to restimulation. Calcium calibrations were performed using *in vitro* standards (Grynkiewicz et al., 1985).

**Cell treatment for *c-fos* induction.** MEM-C growth medium was removed from each culture well and replaced with Hanks' Balanced Salt

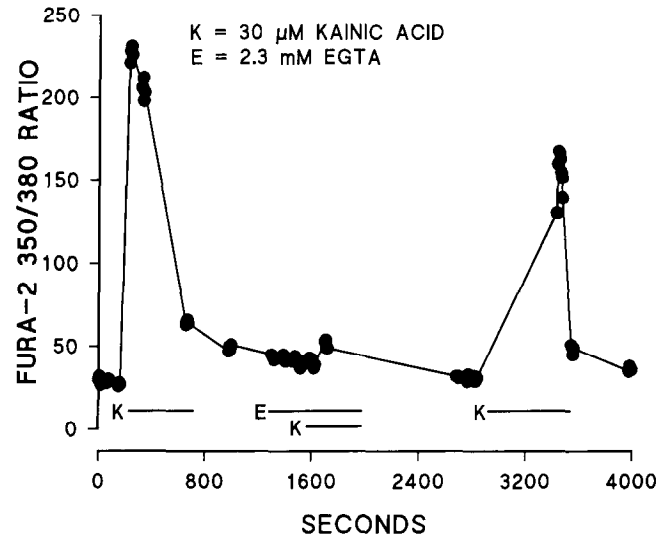


**Figure 3.** Effects of EGTA on the KA-stimulated calcium response. Fura-2-loaded dentate gyrus cells were stimulated with KA ( $30 \mu\text{M}$ ) in the presence of  $\text{Ca}^{2+}$  ( $2 \text{ mM}$ ), rinsed, and allowed to recover for 15 min. The same cells were restimulated with KA in the presence of  $2.3 \text{ mM}$  EGTA. Cells were rinsed, returned to  $\text{Ca}^{2+}$ -containing buffer, allowed to recover, and stimulated a third time with KA. Fura-2 350:380 nm ratios were collected at the times indicated. The bars indicate addition of agonist or drug to the buffer. The fura-2 350/380 ratio refers to the mean, background corrected, 350:380 nm ratio. Values were obtained from cursor boxes placed over ratioed images of single cells.

Solution (HBSS supplemented with  $26 \text{ mM}$   $\text{NaHCO}_3$ ,  $2.3 \text{ mM}$   $\text{CaCl}_2$ ,  $10 \text{ mM}$  HEPES, and  $5 \mu\text{M}$  glycine). Cells were returned to the  $37^\circ\text{C}$  incubator for 3–4 hr prior to stimulation. Cells were incubated with the designated treatment for 30 min at  $37^\circ\text{C}$  unless otherwise stated. Following treatment, cells were fixed with 4% paraformaldehyde at  $4^\circ\text{C}$  for 7–10 min, rinsed with HBSS supplemented with  $10 \text{ mM}$  HEPES, and dehydrated through a series of ethanols. Cells were stored at  $-70^\circ\text{C}$  until used for *in situ* hybridization.

**Oligonucleotide probe.** A 50-base pair oligonucleotide sequence of *c-fos* that exhibited minimal homology with known portions of the rodent genome was chosen. The sequence was complementary to nucleotides 270–319 of rat *c-fos* (Curran et al., 1987). Radiolabeled oligonucleotide was prepared with a 3'-terminal transphosphorylation and  $^{32}\text{P}$ - $\alpha$ -dATP ( $6000 \text{ Ci/mmol}$ ; Du Pont–New England Nuclear) to yield a specific activity of  $2\text{--}4 \times 10^9 \text{ cpm}/\mu\text{g}$ . Evidence that this oligonucleotide hybridizes selectively to *c-fos* mRNA has been previously demonstrated and published by this laboratory (Simonato et al., 1991).

***c-fos* riboprobe.** Antisense and sense *c-fos* riboprobes were prepared from a full-length *c-fos* cDNA insert (generously supplied by J. Morgan and T. Curran, Roche Institute of Molecular Biology, Nutley, NJ). The full-length *c-fos* cDNA insert is cloned in a pSP65 plasmid containing the SP6 promoter and contains a single XhoI restriction site at base 1353 from the 5' end. The plasmid was linearized with XhoI and riboprobes generated using a SP6 transcription assay in the presence of  $^{35}\text{S}$ -rUTP. Antisense and sense riboprobes were hydrolyzed to fragments of approximately 200 base pairs with sodium carbonate at  $60^\circ\text{C}$ .

**In situ hybridization for  $^{32}\text{P}$ -oligonucleotides.** Slides were thawed gradually to room temperature and incubated successively in 95% EtOH, 70% EtOH, and 50% EtOH to rehydrate the cells. Cells were treated with 0.25% acetic anhydride diluted in  $0.1 \text{ M}$  triethanolamine, 0.9% saline for 10 min prior to hybridization. Cells were rinsed briefly in diethylpyrocarbonate-treated water, dehydrated in increasing concentrations of EtOH, and incubated for 3–4 hr at  $37^\circ\text{C}$  in prehybridization buffer [50% formamide;  $0.6 \text{ M}$  NaCl,  $2 \text{ mM}$  EDTA,  $20 \text{ mM}$  Tris ( $2\times$  NTE);  $5\times$  Denhardt's solution (Sigma);  $500 \mu\text{g}/\text{ml}$  yeast tRNA (Sigma);  $500 \mu\text{g}/\text{ml}$  salmon sperm DNA (Sigma); and  $0.05\%$  sodium pyrophosphate]. Cells were hybridized overnight (approximately 16 hr) at  $37^\circ\text{C}$  in the above buffer containing  $100 \mu\text{g}/\text{ml}$  tRNA,  $100 \mu\text{g}/\text{ml}$  DNA, and  $0.025 \text{ ng}/\mu\text{l}$   $^{32}\text{P}$ -labeled *c-fos* oligonucleotide. Nonspecific hybridization of radiolabeled probe to the cells was determined by including unlabeled



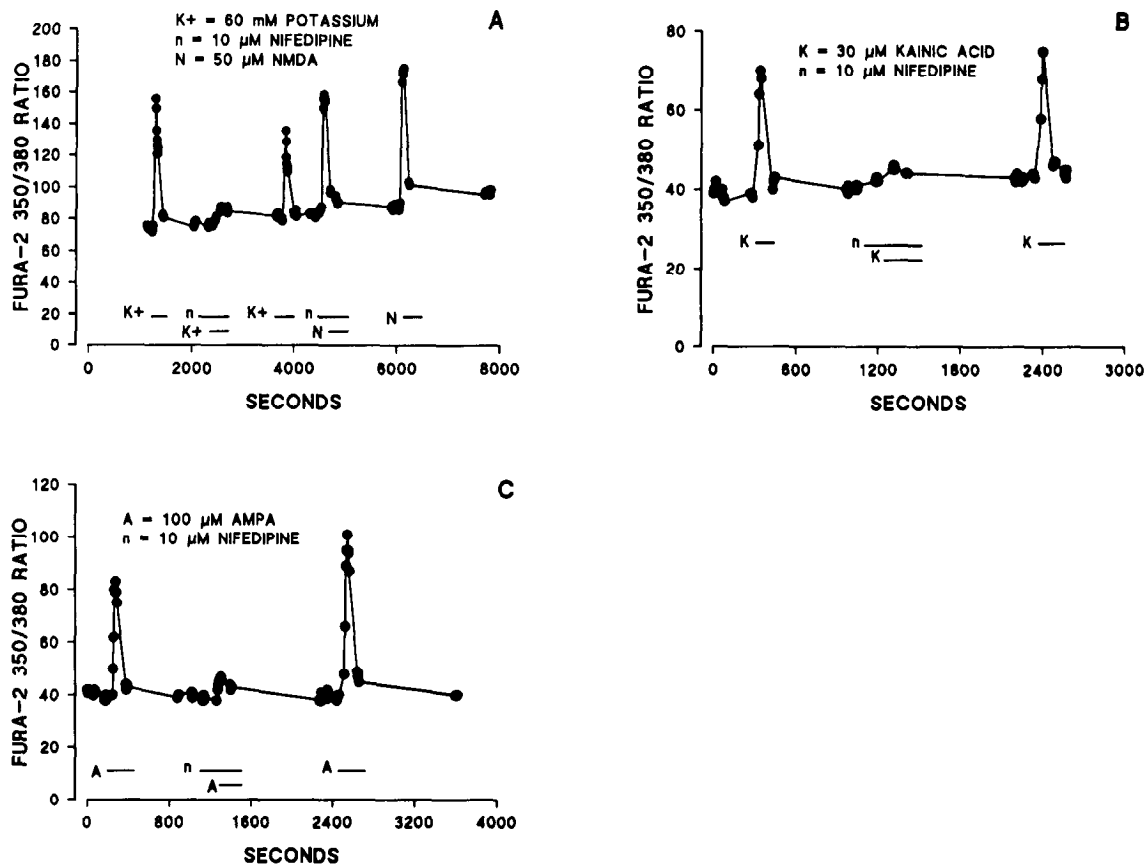


**Figure 4.** Effects of nifedipine on calcium responses to various stimulations. *A*, Fura-2-loaded cells were stimulated with K<sup>+</sup> (60 mM), rinsed, and restimulated with K<sup>+</sup> in the presence of 10 μM nifedipine. Nifedipine was washed out and the same field of cells was stimulated for a third time with 60 mM K<sup>+</sup>. Nifedipine markedly decreased the K<sup>+</sup>-induced Ca<sup>2+</sup> response in a reversible manner. The cells were then stimulated with NMDA (50 μM) in the presence or absence of 10 μM nifedipine. Nifedipine had no effect on the NMDA-mediated Ca<sup>2+</sup> response. The bars indicate drug additions to the extracellular buffer. *B*, Fura-2-loaded cells were pretreated with APV (100 μM) and stimulated with KA (30 μM). Cells were rinsed, allowed to recover, and restimulated with KA in the presence of 10 μM nifedipine. Cells were rinsed and stimulated a third time with KA in the absence of nifedipine. Nifedipine blocked the KA-mediated increase in Ca<sup>2+</sup> in a reversible manner. *C*, Fura-2-loaded cells were pretreated with APV and stimulated with AMPA (100 μM). Cells were rinsed, allowed to recover, and restimulated with AMPA in the presence of 10 μM nifedipine. Cells were rinsed and stimulated a third time with AMPA in the absence of nifedipine. Nifedipine blocked the AMPA-mediated increase in Ca<sup>2+</sup>.

oligonucleotide probe in the prehybridization and hybridization buffer (10× and 100× concentrations, respectively) in adjacent wells. Following hybridization, cells were washed [20 min at room temperature in 1× NTE, 0.05% sodium pyrophosphate; 3 hr at 37°C in 10 mM Tris, 1 mM EDTA, 0.05% sodium pyrophosphate, 75 mM NaCl], dehydrated, and air dried. All slides were dipped in NTB-3 liquid emulsion (Kodak) and stored at 4°C for 17–21 d.

Emulsion-coated slides were developed in Kodak D-19 (4 min), rinsed in water (30 sec), and fixed in Kodak fixer (6 min). Cells were stained for Nissl substance, and silver grains were visualized and counted using either bright-field or dark-field optics on a Leitz Laborlux-12 microscope. Data are presented as silver grains per individual cell.

**In situ hybridization for <sup>35</sup>S-riboprobe.** Slides were treated as above. Cells were incubated for 3–4 hr at 55°C with prehybridization buffer [50% formamide, 10% dextran sulfate, 3× SSC (0.45 M NaCl, 0.045 M citric acid), 5× Denhardt's solution, 500 μg/ml yeast tRNA (Sigma), 500 μg/ml salmon sperm DNA (Sigma), and 10 mM dithiothreitol]. Cells were hybridized overnight (approximately 16 hr) at 55°C in the above buffer containing 60 ng/ml <sup>35</sup>S-labeled antisense riboprobe. Non-specific hybridization was determined by using an <sup>35</sup>S-labeled *c-fos* sense riboprobe in adjacent wells. Following hybridization cells were rinsed with 4× SSC (three times, 15 min each) and RNase treated at 37°C for 30 min. Cells were then rinsed with 2×, 1×, and 0.5× SSC (15 min each) and 0.1× SSC at 55°C for 30 min. All slides were dipped in NTB-3 liquid emulsion and stored at 4°C for 3–5 d. Slides were developed, stained, and quantitated as described above.

## Results

### Characterization of dentate gyrus cells in vitro

An *in vitro* preparation of CNS neurons was used to study changes in Ca<sub>i</sub><sup>2+</sup> and *c-fos* mRNA following EAA receptor stimulation. Dissociation of postnatal dentate gyrus yielded an enriched neuronal population. Neurons were identified morphologically as having small cell somata with several well-defined elongated neurites. This was confirmed by demonstrating that all morphologically identified neurons were immunoreactive with an antibody directed against the 200 kDa neurofilament protein (data not shown). Since dentate gyrus contains both excitatory as well as inhibitory neurons, an antiserum to the enzyme GAD was used to identify the percentage of inhibitory neurons present in the preparation. Less than 5% of the neurofilament-positive neurons stained with antisera directed against GAD (data not shown). Cultures prepared from whole hippocampus were used as positive controls for GAD immunoreactivity. Since the majority of cells are GAD negative (95%) and the dissection includes only the molecular and granule cell layers of the dentate gyrus, our cellular population most likely consists of excitatory granule neurons. We used isolated dentate gyrus neurons for

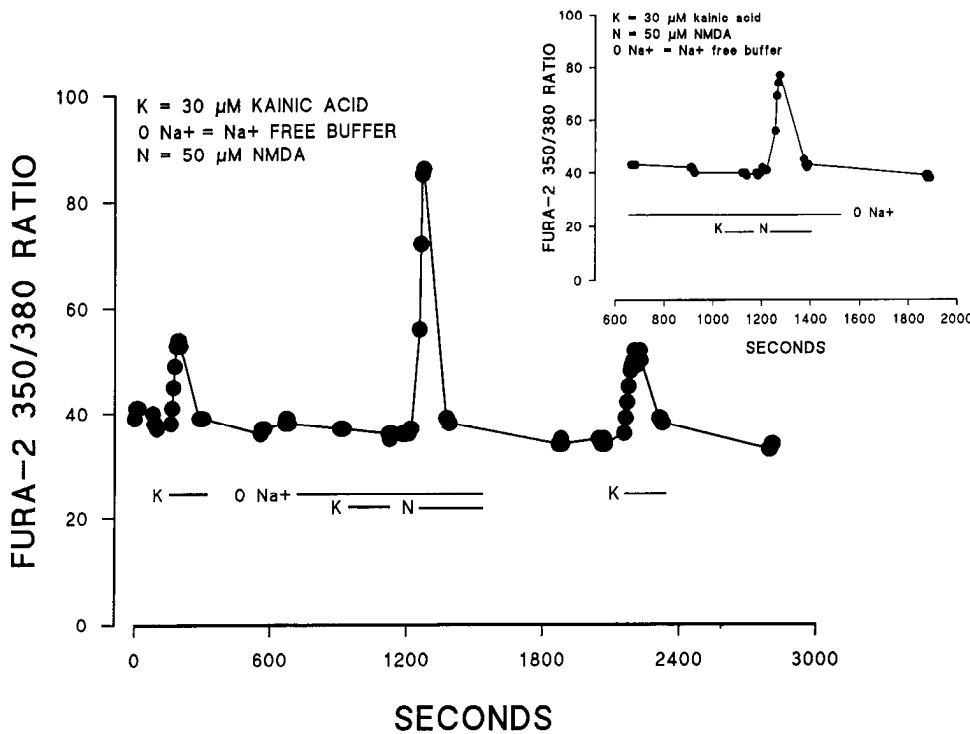


**Figure 5.** Effect of removing  $\text{Na}^+$  on KA- and NMDA-stimulated calcium responses. Fura-2-loaded cells were pretreated with APV ( $100 \mu\text{M}$ ) and stimulated with KA ( $30 \mu\text{M}$ ) in HBSS. Cells were rinsed and allowed to recover before being placed in  $\text{Na}^+$ -free buffer (sodium replaced with an equimolar concentration of NMDG). Cells were first stimulated with KA in the  $\text{Na}^+$ -free environment. No increase in  $\text{Ca}^{2+}$  occurred in response to KA in the  $\text{Na}^+$ -free environment. Cells were then stimulated with  $50 \mu\text{M}$  NMDA while still in the  $\text{Na}^+$ -free buffer; NMDA stimulation yielded a dramatic rise in  $\text{Ca}^{2+}$  under these same conditions. Cells were rinsed, allowed to recover in buffer containing  $\text{Na}^+$ , and restimulated with KA, yielding a normal  $\text{Ca}^{2+}$  response. *Inset*, An expanded time course of the  $\text{Ca}^{2+}$  responses following KA and NMDA in  $\text{Na}^+$ -free buffer. The bars indicate the additions of agonists to, or changes in, the extracellular buffer.

these studies because these neurons exhibit robust *c-fos* mRNA in a variety of paradigms *in vivo* (Morgan et al., 1987; Sonnenberg et al., 1989; Simonato et al., 1991). Non-neuronal cells were polygonal in shape and were identified as astroglia by immunocytochemical staining with antisera to GFAP.

#### Intracellular calcium responses to EAA receptor agonists

Changes in  $\text{Ca}_i^{2+}$  following bath application of EAA receptor agonists or depolarizing concentrations of potassium ( $\text{K}^+$ ) were monitored in individual dentate gyrus cells using the  $\text{Ca}^{2+}$ -sensitive dye fura-2. Neurons ( $n = 75$ ) stimulated with NMDA exhibited a rapid increase in the fura-2 350:380 nm ratio, indicating an increase in  $\text{Ca}_i^{2+}$  (Fig. 1). The basal  $\text{Ca}_i^{2+}$  concentration ranged from 50 to 70 nM and increased to a maximum of 300–400 nM after NMDA application. Intracellular  $\text{Ca}^{2+}$  remained elevated as long as the agonist was present (2 min maximum time tested) and returned to basal levels upon NMDA washout. Non-neuronal cells were never observed to respond to NMDA.

The NMDA-induced increase in  $\text{Ca}_i^{2+}$  was dependent on the presence of extracellular calcium ( $\text{Ca}_e^{2+}$ ). NMDA-mediated increases in  $\text{Ca}_i^{2+}$  were markedly inhibited by either chelation of  $\text{Ca}_e^{2+}$  with EGTA (1 mM; Fig. 2A) or omission of  $\text{Ca}_e^{2+}$  from the extracellular buffer (Fig. 2B). This inhibition was reversed upon returning the cells to  $\text{Ca}_e^{2+}$ -containing buffer. The non-NMDA receptor selective agonists kainic acid (KA;  $30 \mu\text{M}$ ) and AMPA ( $\alpha$ -amino-3-hydroxy-5-methyl-4-isoxazolepropionic acid;  $100 \mu\text{M}$ ) also rapidly increased  $\text{Ca}_i^{2+}$  (see below); this  $\text{Ca}_i^{2+}$  response was also blocked by addition of EGTA to the extracellular buffer (Fig. 3). NMDA was applied in the presence of  $10 \mu\text{M}$  CNQX (6-cyano-7-nitroquinoxaline-2,3-dione) to block non-NMDA receptors; non-NMDA receptor agonists were applied in the presence of APV [ $\text{D}(-)$ -2-amino-5-phosphonopentanoic acid] to block NMDA receptor activation.

#### Effects of nifedipine on calcium responses to EAA receptor agonists

The NMDA receptor is permeable to  $\text{Ca}^{2+}$  as well as to  $\text{Na}^+$  and  $\text{K}^+$  (Macdermott et al., 1986). NMDA receptor activation may therefore induce  $\text{Ca}^{2+}$  influx directly through the receptor channel itself as well as indirectly through voltage-sensitive calcium channels (VSCCs) activated in response to receptor-mediated cell depolarization. Nifedipine, a dihydropyridine  $\text{Ca}^{2+}$  channel blocker, was used to distinguish between these two sites of  $\text{Ca}^{2+}$  influx. Blocking dihydropyridine-sensitive voltage-dependent  $\text{Ca}^{2+}$  channels with nifedipine ( $10 \mu\text{M}$ ) did not inhibit NMDA-induced increases in  $\text{Ca}_i^{2+}$ . In contrast, nifedipine markedly inhibited the  $\text{Ca}_i^{2+}$  responses to KA, AMPA, and depolarizing concentrations of  $\text{K}^+$  (Fig. 4A–C). The remaining small  $\text{Ca}_i^{2+}$  response observed in the presence of nifedipine may be due to  $\text{Ca}^{2+}$  influx through nifedipine-insensitive VSCCs or influx through non-NMDA channels directly. The role of VSCCs was further tested by replacing  $\text{Na}_e^+$  with the nonpermeable cation *N*-methyl-D-glucamine (NMDG) to decrease agonist-induced depolarization. The NMDA-induced  $\text{Ca}_i^{2+}$  response was not affected by the removal of  $\text{Na}_e^+$ , whereas the  $\text{Ca}_i^{2+}$  response following KA stimulation was inhibited (Fig. 5). Together with the results found with nifedipine, these results suggest that the principal route of  $\text{Ca}^{2+}$  entry following NMDA application is through the NMDA receptor itself and does not require activation of VSCCs. In contrast, in this preparation the non-NMDA receptor agonists primarily rely on the opening of VSCCs for the influx of  $\text{Ca}_i^{2+}$ .

#### Induction of *c-fos* mRNA by EAA receptor agonists

Dentate gyrus cells maintained *in vitro* were used to study EAA induction of *c-fos* mRNA. NMDA induced *c-fos* mRNA 10–15-fold over basal levels in individual neurons ( $n = 765$ ). NMDA

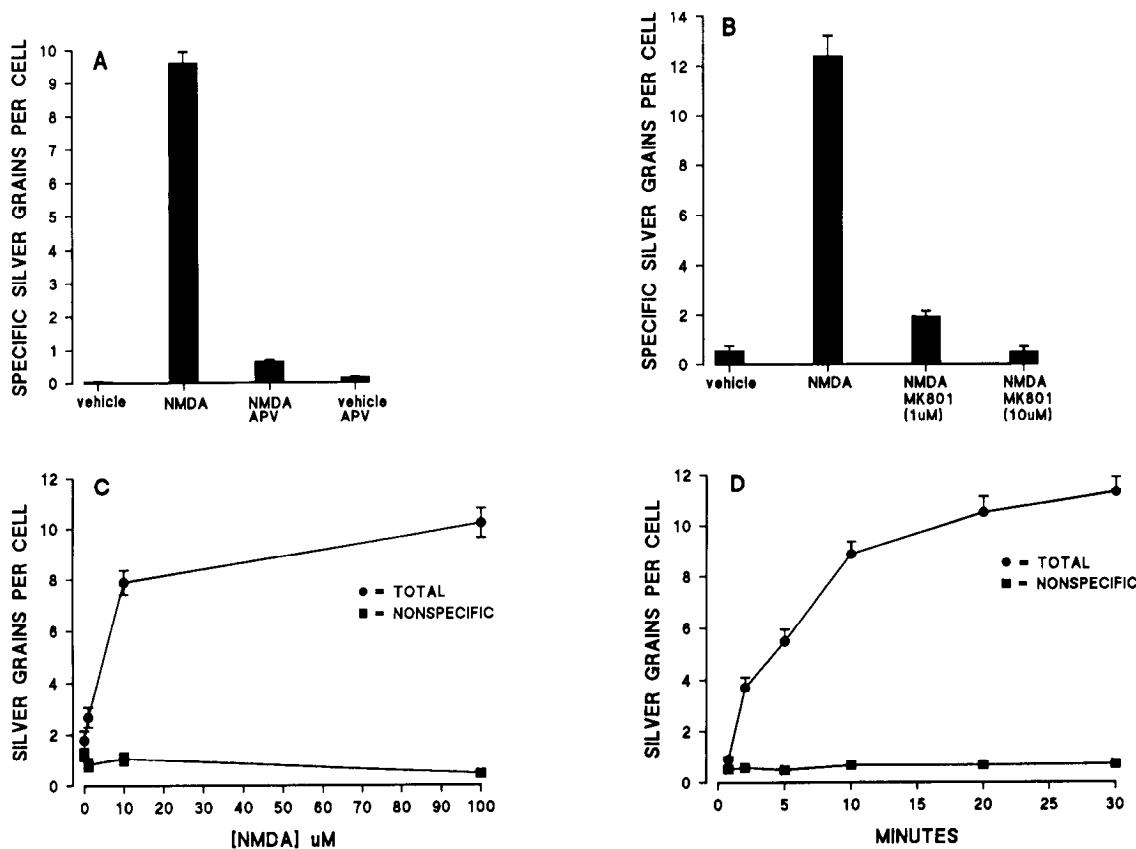


**Figure 6.** NMDA-stimulated changes in *c-fos* mRNA in cultured dentate gyrus cells. All cells were stimulated for 30 min and processed for *in situ* hybridization as described in Materials and Methods. Silver grains were counted over individual cells. *A* and *B*, *c-fos* mRNA in dentate cells stimulated with NMDA (50  $\mu$ M) in the absence or presence of APV (*A*) or Mk-801 (*B*). Each data point comes from at least 50 individual neurons. *C*, Dose-response curve of NMDA-induced *c-fos* mRNA. Cells were incubated with varying concentrations of NMDA for 30 min. Data are from a single representative experiment, repeated three times. The response at each dose is determined from counting silver grains over at least 20 individual neurons. *D*, Time course of NMDA-induced *c-fos* mRNA expression. Cells were treated with 50  $\mu$ M NMDA for varying times. APV was added at the appropriate times to block NMDA receptor activation. Cells were fixed 30 min after the initial addition of NMDA. Data are from a single representative experiment, repeated at least three times. Data for each time point are from at least 50 individual neurons. Error bars refer to  $\pm$ SEM.

induction of *c-fos* mRNA was blocked by the competitive NMDA receptor antagonist APV (100  $\mu$ M) as well as the noncompetitive antagonist Mk-801 (1  $\mu$ M, 10  $\mu$ M; Fig. 6*A,B*). Induction of *c-fos* mRNA occurred in a dose-dependent manner with near-maximal expression being reached with 10  $\mu$ M NMDA (Fig. 6*C*). *c-fos* mRNA induction by NMDA was reduced to basal levels by chelating  $Ca^{2+}$  with EGTA, suggesting that  $Ca^{2+}$  influx from the extracellular environment is required for the response (Fig. 7*D*).

The NMDA induction of *c-fos* mRNA was time dependent with near-maximal increases observed after a 10 min exposure (Fig. 6*D*). A 1–3 min exposure to 50  $\mu$ M NMDA was sufficient to induce an increase in *c-fos* mRNA detected 30 min after agonist exposure (Fig. 8). Shorter exposure times to NMDA (30 and 45 sec) did not result in an increase in *c-fos* mRNA, even though this did result in clear increases of  $Ca^{2+}$  (Fig. 8, inset).

Non-NMDA receptor agonists also induce *c-fos* mRNA in individual dentate neurons. AMPA (100  $\mu$ M;  $n = 50$ ) and KA (30  $\mu$ M;  $n = 141$ ) induce *c-fos* mRNA 10–15-fold over basal (Fig. 7*A,B*). Depolarizing the cells directly with  $K^+$ , in the presence of receptor antagonists, also results in an increase in *c-fos* mRNA (60 mM;  $n = 161$ ). *c-fos* mRNA induction following KA was also  $Ca^{2+}$  dependent, the response being reduced to basal levels by chelating  $Ca^{2+}$  with EGTA (Fig. 7*C*).

#### Effects of nifedipine on *c-fos* induction

Nifedipine blocked the induction of *c-fos* mRNA by  $K^+$  and KA, whereas it had little effect on NMDA-mediated *c-fos* induction (Fig. 9*A–C*). Nifedipine also blocked AMPA-induced *c-fos* mRNA (data not shown). These results correlate well with the  $Ca^{2+}$  data presented above where NMDA stimulation increased  $Ca^{2+}$  even in the presence of nifedipine. These findings suggest that NMDA-mediated induction of *c-fos* mRNA requires  $Ca^{2+}$  influx directly through the NMDA channel.

#### Discussion

Three principal findings emerge from this study. (1) Activation of either NMDA or non-NMDA subtypes of EAA receptors is sufficient to induce the rapid and dramatic increase of *c-fos* mRNA in isolated dentate gyrus neurons. (2) *c-fos* mRNA induction by either receptor subtype requires an increase of  $Ca^{2+}$ . Receptor-mediated increases of both  $Ca^{2+}$  and *c-fos* mRNA are blocked by chelation of  $Ca^{2+}$  with EGTA. (3) The increases of  $Ca^{2+}$  and *c-fos* mRNA triggered by KA or AMPA, but not NMDA, are prevented by nifedipine, a VSCC blocker.

Our results are consistent with the report by Szekely et al. (1989) in which NMDA receptor activation induced *c-fos* mRNA in cultured cerebellar granule cells. We extend those observa-

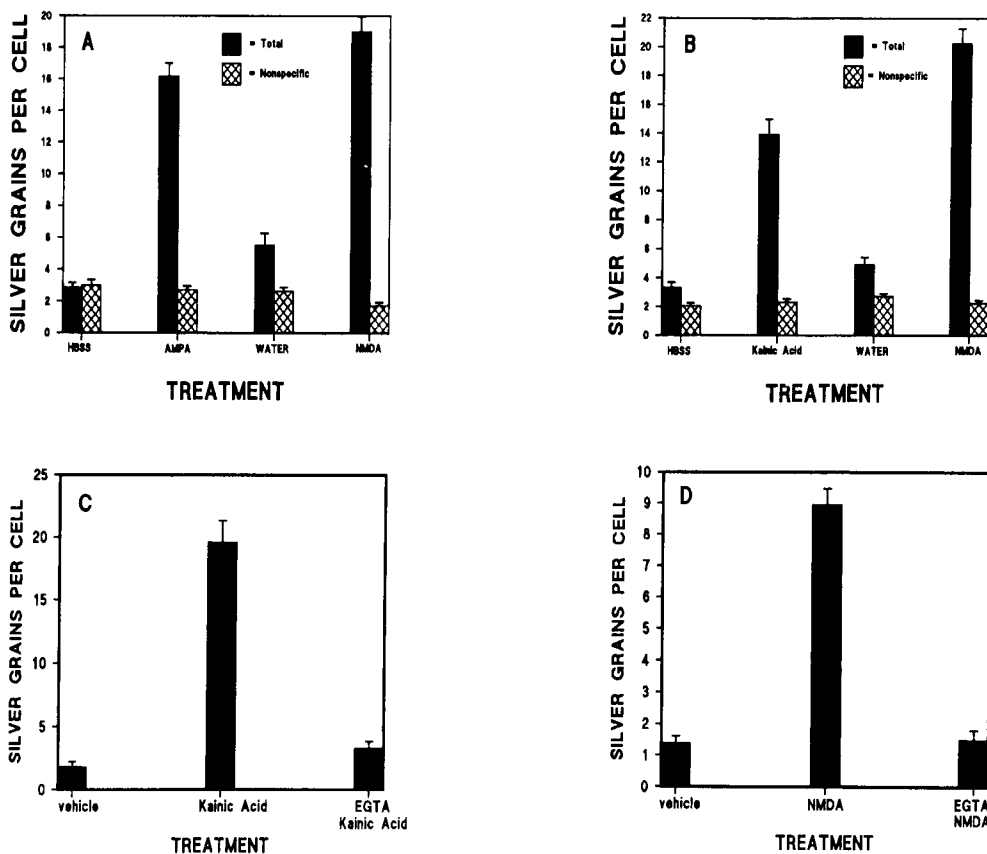


**Figure 7.** KA and AMPA stimulated changes in *c-fos* mRNA in dentate gyrus cells. Cells were pretreated with 100  $\mu$ M APV to block NMDA receptors prior to adding KA or AMPA. *A* and *B*, *c-fos* mRNA in response to 100  $\mu$ M AMPA (*A*) or 30  $\mu$ M KA (*B*). Water is the vehicle used for KA and AMPA; HBSS is the vehicle used for NMDA. Each experiment was repeated at least three times. Each data point comes from counting silver grains over at least 50 individual neurons. Data from NMDA (50  $\mu$ M)-stimulated cells maintained in adjacent wells on the same slides are included in each panel as a positive control for the induction of *c-fos* mRNA. *C* and *D*, *c-fos* mRNA in response to 30  $\mu$ M KA (*C*) or 50  $\mu$ M NMDA (*D*) in the absence and presence of 2.3 mM EGTA. Water is the vehicle used for KA; HBSS is the vehicle used for NMDA. Chelation of  $Ca^{2+}$  with EGTA blocked the induction of *c-fos* mRNA by both KA and NMDA. Each experiment was repeated three times. Error bars refer to  $\pm$ SEM.

tions by demonstrating the absolute requirement for  $Ca^{2+}$  in the NMDA-mediated response. Our results differ from Szekely et al. (1989) in that KA is also sufficient to induce *c-fos* mRNA in dentate gyrus neurons whereas it was ineffective in cerebellar

granule cells. Whether a reduced expression of KA/AMPA receptor subtypes, a difference in VSCCs or some other factor unique to the cerebellar granule cell preparation accounts for this difference is unknown.

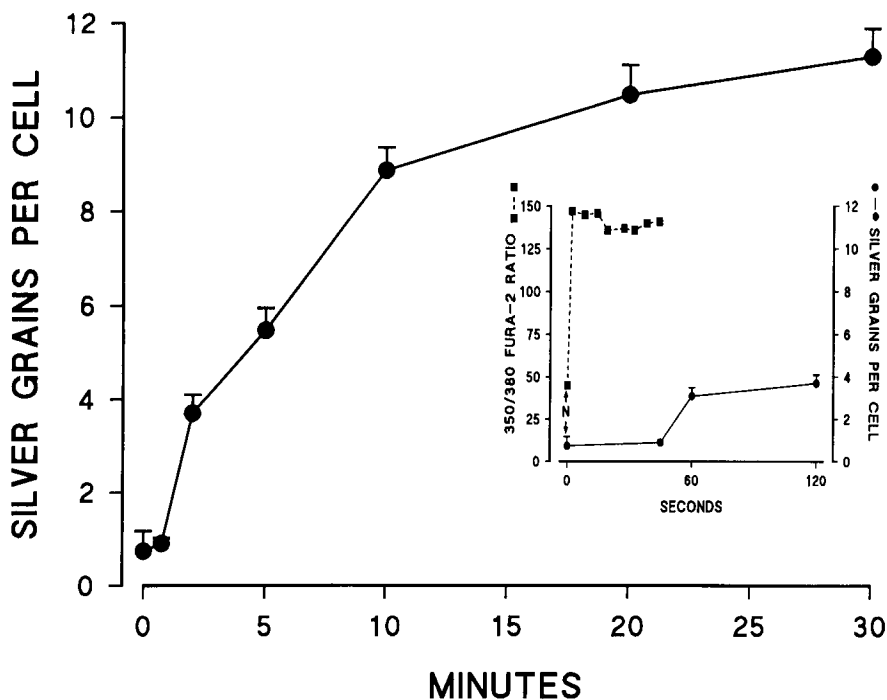


**Figure 8.** Time course of NMDA-mediated increase in *c-fos* mRNA and intracellular calcium. Dentate gyrus neurons were treated with NMDA and processed for *in situ* hybridization to detect *c-fos* mRNA or fura-2 imaging to detect changes in  $Ca^{2+}$  as described in Materials and Methods. NMDA treatment caused an increase in *c-fos* mRNA in a time-dependent manner. Exposure to NMDA for less than 1 min did not result in an increase in *c-fos* mRNA (same data shown in Fig. 6D). *Inset*, Fura-2  $Ca^{2+}$  responses and *c-fos* mRNA responses plotted on the same graph following up to 2 min of NMDA treatment. *N* indicates the addition of 50  $\mu$ M NMDA. For  $Ca^{2+}$  responses, changes in the fura-2 ratio were monitored immediately following addition of NMDA. For *c-fos* mRNA detection, cells were exposed to NMDA for various times from 0 to 120 sec followed by addition of APV to block continued receptor activation. Cells were incubated for 30 min prior to being fixed and processed for *in situ* hybridization. The increase in  $Ca^{2+}$  following NMDA addition was immediate and sustained for as long as agonist was present. In contrast, exposure to NMDA for less than 1 min did not induce *c-fos* mRNA. Error bars refer to  $\pm$ SEM.

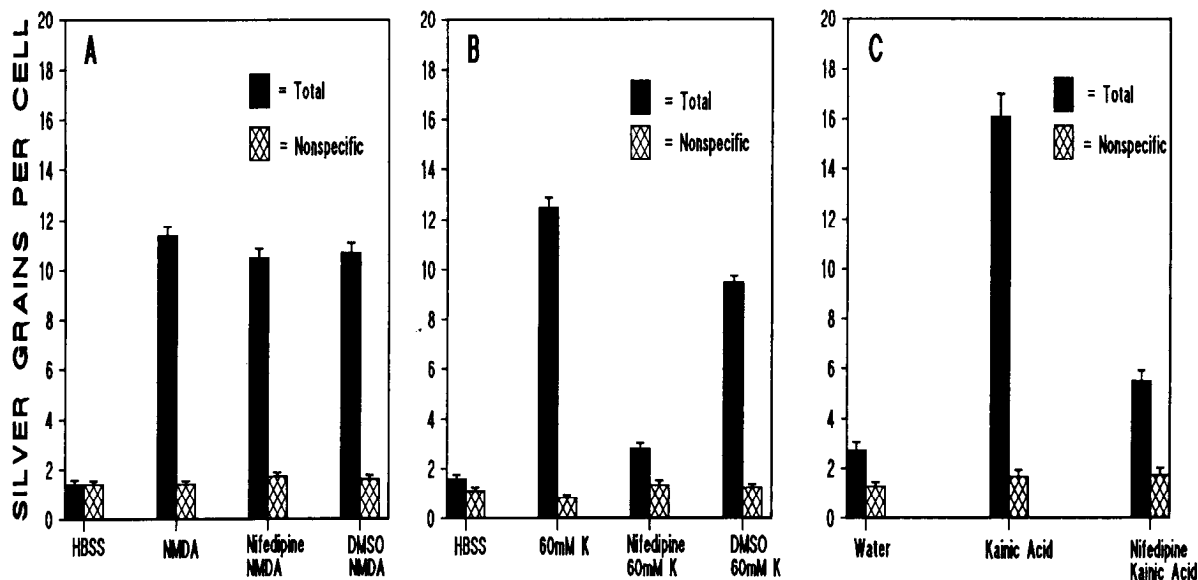


**Figure 9.** Effect of nifedipine on stimulated changes in *c-fos* mRNA in dentate cells. Cells were processed for *in situ* hybridization to detect *c-fos* mRNA as described in Materials and Methods. Non-NMDA receptor agonists and  $K^+$  were added in the presence of APV to block NMDA receptor activation. **A**, Cells were stimulated with NMDA ( $50 \mu\text{M}$ ) in the absence or presence of nifedipine ( $10 \mu\text{M}$ ). Nifedipine was dissolved in dimethyl sulfoxide and diluted into HBSS. Each data point comes from counting silver grains over at least 70 individual neurons. Nifedipine did not decrease the NMDA induction of *c-fos* mRNA. **B**, Cells were stimulated with  $60 \text{ mM } K^+$  in the absence or presence of nifedipine ( $10 \mu\text{M}$ ). Each data point comes from counting silver grains over at least 70 individual neurons. Nifedipine blocked the  $K^+$ -induced increase of *c-fos* mRNA. **C**, Cells were stimulated with  $30 \mu\text{M}$  KA in the absence or presence of nifedipine ( $10 \mu\text{M}$ ). Each data point comes from counting silver grains over at least 50 individual neurons. Nifedipine blocked the KA induction of *c-fos* mRNA. Error bars refer to  $\pm$ SEM.

Interestingly, NMDA-induced rises in  $Ca^{2+}$  of  $<1$  min did not induce *c-fos* mRNA. A sustained NMDA-induced increase in  $Ca^{2+}$  was required for the maximal induction of *c-fos* mRNA, 10 min of NMDA stimulation resulting in a more than twofold greater induction of *c-fos* mRNA compared to a 2 min stimulation. Our data demonstrate that a transient  $Ca^{2+}$  rise alone is not sufficient for the direct induction of *c-fos* mRNA, but more likely a sustained increase in  $Ca^{2+}$  is necessary. Sustained increases in  $Ca^{2+}$  lasting several minutes occur in hippocampal CA3 cells following a train of electrical stimuli (Muller and Connor, 1991), as well as in hippocampal CA1 cells following focal NMDA (Connor et al., 1988). Our findings may help explain the low constitutive expression of *c-fos* mRNA in normal rat brain where sustained increases in  $Ca^{2+}$  presumably are not occurring under physiologic conditions. The nature of the signaling mechanisms activated by the sustained  $Ca^{2+}$  rises is presently unclear.

Previous work from this laboratory indicated that NMDA receptor antagonists inhibited kindled seizure induction of *c-fos* mRNA in dentate granule cells by 50–70% (Labiner et al., 1990). Such results suggest that NMDA receptor activation is necessary for the full expression of seizure-induced *c-fos* mRNA. The present findings demonstrate that NMDA receptor activation is sufficient to induce *c-fos* mRNA and that  $Ca^{2+}$  is an essential second messenger in this signaling cascade. Our results suggest that synaptically released glutamate during a seizure could evoke an increase of *c-fos* mRNA by activating either NMDA or non-NMDA receptor subtypes. This could account for the residual 30–50% of *c-fos* mRNA found in the presence of NMDA antagonists (Labiner et al., 1990).

Our data indicate that the route of  $Ca^{2+}$  entry into dentate gyrus neurons differs following KA/AMPA and NMDA receptor activation. KA-induced increases in  $Ca^{2+}$  can be eliminated by

nifedipine or by substituting  $Na^+$  with NMDG, suggesting that  $Ca^{2+}$  enters the neurons principally through VSCCs activated by neuronal depolarization. Although  $Ca^{2+}$  influx directly through non-NMDA receptors has recently been reported (Gilbertson et al., 1991; Hollmann et al., 1991), we do not detect significant  $Ca^{2+}$  influx directly through KA/AMPA receptors in these neurons as measured with fura-2 imaging. In contrast, NMDA receptor activation appears to evoke  $Ca^{2+}$  entry primarily through the NMDA receptor directly. Sodium ions account for approximately 88% of the depolarizing current induced by NMDA in neurons (Mayer and Westbrook, 1987). Removal of  $Na^+$  should therefore greatly attenuate the depolarizing current following NMDA stimulation. The persistent NMDA-induced increase of  $Ca^{2+}$  in the presence of the nonpermeable cation NMDG, as well as in the presence of nifedipine, suggests that the majority of  $Ca^{2+}$  enters directly through the NMDA receptor, not indirectly through VSCCs.

Although the routes of  $Ca^{2+}$  entry differ following activation of non-NMDA and NMDA receptors, the rise of  $Ca^{2+}$  triggered by each receptor induces a dramatic increase in *c-fos* mRNA. The colocalization of non-NMDA and NMDA receptors at individual synapses (Bekkers and Stevens, 1989; Jones and Baughman, 1991) together with these findings suggests that synaptically released glutamate could trigger induction of *c-fos* mRNA by  $Ca^{2+}$  entering a cell via two distinct routes. The preponderance of VSCCs in the vicinity of the cell soma and proximal dendrites (Lipscombe et al., 1988; Westenbroek et al., 1990), and of NMDA receptors in the dendrites (Monaghan and Cotman, 1985; Jones and Baughman, 1991), suggests that increases in  $Ca^{2+}$  may be spatially separate within the cell (Tank et al., 1988; Regehr and Tank, 1990). Muller and Connor (1991) have recently demonstrated regional changes in  $Ca^{2+}$  levels within individual hippocampal cells following electrical stimulation.



Despite potentially distinct pools of elevated  $\text{Ca}_i^{2+}$  resulting from activation of each receptor, the increases of *c-fos* mRNA may reflect the independent activation of identical genetic programs, providing redundancy in the genetic consequences. Alternatively, it has previously been demonstrated that increases in  $\text{Ca}_i^{2+}$  arising from distinct sources can trigger different biochemical responses (Brooks et al., 1989). Such differences could lead to the induction of distinct arrays of IEGs, *c-fos* mRNA being common to each. If so, distinct arrays of IEGs could regulate expression of distinct arrays of target genes, thereby effecting unique and receptor subtype-specific long-term phenotypic consequences.

## References

- Aniksztejn L, Ben-Ari Y (1991) Novel form of long-term potentiation produced by a  $\text{K}^+$  channel blocker in the hippocampus. *Nature* 349:67–69.
- Ascher P, Nowak L (1988) The role of divalent cations in the *N*-methyl-D-aspartate responses of mouse central neurons in culture. *J Physiol (Lond)* 399:247–266.
- Bekkers JM, Stevens CF (1989) NMDA and non-NMDA receptors are co-localized at individual excitatory synapses in cultured rat hippocampus. *Nature* 341:230–233.
- Brooks RC, McCarthy KD, Lapetina EG, Morell P (1989) Receptor-stimulated phospholipase A<sub>2</sub> activation is coupled to influx of external calcium and not to mobilization of intracellular calcium in C62B glioma cells. *J Biol Chem* 264:20147–20153.
- Collingridge GL, Kehl SJ, McLennan H (1983) Excitatory amino acids in synaptic transmission in the Schaffer collateral-commissural pathway of the rat hippocampus. *J Physiol (Lond)* 334:33–46.
- Connor JA, Wadman WJ, Hockberger PE, Wong RK (1988) Sustained dendritic gradients of  $\text{Ca}^{++}$  induced by excitatory amino acids in CA1 hippocampal neurons. *Science* 240:649–653.
- Curran T, Morgan JI (1985) Superinduction of *c-fos* by nerve growth factor in the presence of peripherally active benzodiazepines. *Science* 229:1265–1268.
- Curran T, Gordon MB, Rubino KL, Sambucetti LC (1987) Isolation and characterization of the *c-fos* (rat) cDNA and analysis of post-translational modification *in vitro*. *Oncogene* 2:79–84.
- Dragunow M, Robertson HA (1987) Kindling stimulation induces *c-fos* protein(s) in granule cells of the rat dentate gyrus. *Nature* 329:441–442.
- Gilbertson TA, Scobey R, Wilson M (1991) Permeation of calcium ions through non-NMDA glutamate channels in retinal bipolar cells. *Science* 251:1613–1615.
- Goelet P, Castellucci VF, Schacher S, Kandel ER (1986) The long and the short of long-term memory—a molecular framework. *Nature* 322:419–422.
- Grynkiewicz G, Poenie M, Tsien RY (1985) A new generation of calcium indicators with greatly improved fluorescence properties. *J Biol Chem* 260:3440–3445.
- Harris EW, Ganong A, Cotman CW (1984) Long-term potentiation in the hippocampus involves activation of *N*-methyl-D-aspartate receptors. *Brain Res* 323:132–137.
- Herrera DG, Robertson HA (1990) *N*-methyl-D-aspartate receptors mediate activation of the *c-fos* proto-oncogene in a model of brain injury. *Neuroscience* 35:273–281.
- Hollmann M, Hartley M, Heinemann S (1991)  $\text{Ca}^{++}$  permeability of KA-AMPA-gated glutamate receptor channels depends on subunit composition. *Science* 252:851–853.
- Iino M, Ozawa S, Tsuzuki K (1990) Permeation of calcium through excitatory amino acid receptor channels in cultured rat hippocampal neurons. *J Physiol (Lond)* 424:151–165.
- Jones KA, Baughman RW (1991) Both NMDA and non-NMDA subtypes of glutamate receptors are concentrated at synapses on cerebral cortical neurons in culture. *Neuron* 7:593–603.
- Labiner DM, Hosford DA, Shin C, Cao Z, Butler LS, McNamara JO (1990) Dissociation of neuronal activity and seizure-induced *c-fos* mRNA expression by NMDA receptor antagonist. *Soc Neurosci Abstr* 16:848.
- Lerea LS, McCarthy KD (1990) Neuron-associated astroglial cells express  $\beta$ - and  $\alpha_1$ -adrenergic receptors *in vitro*. *Brain Res* 521:7–14.
- Lipscombe D, Madison DV, Poenie M, Reuter H, Tsien RY, Tsien RW (1988) Spatial distribution of calcium channels and cytosolic calcium transients in growth cones and cell bodies of sympathetic neurons. *Proc Natl Acad Sci USA* 85:2398–2402.
- Macdermott AB, Mayer ML, Westbrook GL, Smith SJ, Barker JL (1986) NMDA-receptor activation increases cytoplasmic calcium concentration in cultured spinal cord neurons. *Nature* 321:519–522.
- Mattson MP, Kater SB (1989) Development and selective neurodegeneration in cell cultures from different hippocampal regions. *Brain Res* 490:110–125.
- Mayer ML, Westbrook GL (1987) Permeation and block of *N*-methyl-D-aspartic acid receptor channels by divalent cations in mouse cultured central neurones. *J Physiol (Lond)* 394:501–527.
- McCarthy KD, Salm AK (1991) Pharmacologically-distinct subsets of astroglia can be identified by their calcium response to neuroleptands. *Neuroscience* 41:325–333.
- McNamara JO, Russell RD, Riggsbee L, Bonhaus DW (1988) Anticonvulsant and antiepileptogenic actions of Mk801 in the kindling and electroshock models. *Neuropharmacology* 27:563–568.
- Monaghan DT, Cotman CW (1985) Distribution of *N*-methyl-D-aspartate-sensitive L-[<sup>3</sup>H]glutamate binding sites in rat brain. *J Neurosci* 5:2909–2919.
- Morgan JI, Curran T (1986) Role of ion flux in the control of *c-fos* expression. *Nature* 322:552–555.
- Morgan JI, Curran T (1989) Stimulus-transcription coupling in neurons: role of cellular immediate-early genes. *Trends Neurosci* 12:459–462.
- Morgan JI, Cohen DR, Hempstead JL, Curran T (1987) Mapping patterns of *c-fos* expression in the central nervous system after seizure. *Science* 237:192–197.
- Muller W, Connor JA (1991) Dendritic spines as individual neuronal compartments for synaptic  $\text{Ca}^{2+}$  responses. *Nature* 354:73–76.
- Regehr WG, Tank DW (1990) Postsynaptic NMDA receptor-mediated calcium accumulation in hippocampal CA1 pyramidal cell dendrites. *Nature* 345:807–810.
- Shin C, McNamara JO, Morgan JI, Curran T, Cohen DR (1990) Induction of *c-fos* mRNA expression by afterdischarge in the hippocampus of naive and kindled rats. *J Neurochem* 55:1050–1055.
- Simonato M, Hosford D, Labiner D, Shin C, Mansbach HH, McNamara JO (1991) Differential expression of immediate early genes in the hippocampus in the kindling model of epilepsy. *Mol Brain Res* 11:115–124.
- Sonnenberg JL, Mitchelmore C, Macgregor-Leon PF, Hempstead J, Morgan JI, Curran T (1989) Glutamate receptor agonists increase the expression of Fos, Fra, and AP-1 DNA binding activity in the mammalian brain. *J Neurosci Res* 24:72–80.
- Stasheff SF, Anderson WW, Clark S, Wilson WA (1989) NMDA antagonists differentiate epileptogenesis from seizure expression in an *in vitro* model. *Science* 245:648–651.
- Szekely AM, Barbaccia ML, Alho H, Costa E (1989) In primary cultures of cerebellar granule cells the activation of *N*-methyl-D-aspartate-sensitive glutamate receptors induces *c-fos* mRNA expression. *Mol Pharmacol* 35:401–408.
- Tank DW, Sugimori M, Connor JA, Llinas RR (1988) Spatially resolved calcium dynamics of mammalian purkinje cells in cerebellar slice. *Science* 242:773–777.
- Westenbroek RE, Ahljianian MK, Catterall WA (1990) Clustering of L-type  $\text{Ca}^{2+}$  channels at the base of major dendrites in hippocampal pyramidal neurons. *Nature* 347:281–284.